Research on
Engineering
Structures & Materials
journal homepage: http://jresm.org

MIM RESEARCH GROUP

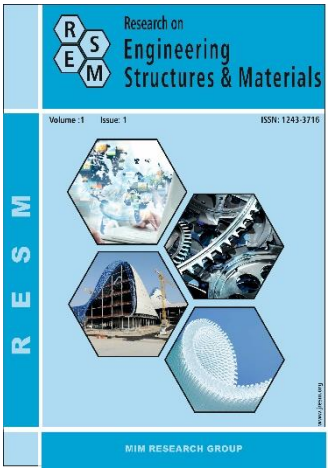

On self-equilibrium state of V-expander tensegrity beam-like grids

Pilade Foti, Aguinaldo Fraddosio, Salvatore Marzano, Gaetano Pavone, Mario Daniele Piccioni

Online Publication Date: 1 Apr 2017
URL: http://dx.doi.org/10.17515/resm2016.81st0727.html
DOI: http://dx.doi.org/10.17515/resm2016.81st0727

Journal Abbreviation: *Res. Eng. Struct. Mat.*

To cite this article
Foti P, Fraddosio A, Marzano S, Pavone G, Piccioni MD. On self-equilibrium state of V-expander tensegrity beam-like grids. *Res. Eng. Struct. Mat.*, 2018; 4(1): 15-34.

Research on Engineering Structures & Materials
journal homepage: http://jresm.org
MIM RESEARCH GROUP

Research Article

On self-equilibrium state of V-expander tensegrity beam-like grids

Pilade Foti[1], Aguinaldo Fraddosio[1], Salvatore Marzano[1], Gaetano Pavone[*,1], Mario Daniele Piccioni[1]

[1]*Dipartimento di Scienze dell'Ingegneria Civile e dell'Architettura, Politecnico di Bari, Bari, ITALIA*

Article Info

Article history:
Received 27 July 2016
Revised 22 Mar 2017
Accepted 1 Apr 2017

Keywords:
Tensegrity system, Self-equilibrium, Force density method, Numerical methods

Abstract

Tensegrity structures are an innovative class of lightweight structures, which have gained the interest of researchers in many different fields, including but not limited to engineering. In particular, such interest is due to their aesthetic value, their large stiffness-to-mass ratio, the possible deployability, together to their reliability and controllability. Tensegrity structures, made of struts in compression and cables necessarily in tension, are innovative structures by itself: they are similar only in appearance to conventional pin-joint structures (trusses), and their mechanical behavior is strongly related to initial feasible self-stress states induced in absence of external loads. In particular, from a kinematical point of view, these self-stress states avoid the activation of possible infinitesimal mechanisms. In this paper, we study an innovative class of tensegrity beam-like grids, obtained by a suitable assembly of three elementary V-Expander tensegrity cells along a longitudinal axis (named *x*-axis) in the three-dimensional space. In particular, by means of a numerical study, we analyze the feasible self-stress states for seven tensegrity beam-like grids, with increasing degree of complexity, made by an arrangement of V-Expander elementary cells. Moreover, we analyze the influence on the feasible self-stress states of the addition of elements starting from the simplest V-Expander tensegrity configuration.

1. Introduction

Tensegrity systems are an innovative class of lightweight structures, which have gained the interest of researchers in many different fields, including but not limited to engineering. In particular, the interest for tensegrity structures in structural engineering as well as in architecture is due to their aesthetic value, and to their large stiffness-to-mass ratio. Thus, the tensegrity concept has found applications such as towers, large dome structures, stadium roofs, temporarily structures and tents [1, 2]. Furthermore, the folding and the deployment capabilities of these systems may allow the use of tensegrity systems for producing deployable structures, with promising future applications [3, 4].

Tensegrity structures are pin-connected free-standing frameworks composed of struts in compression and cables necessarily in tension [5, 6]. Tensegrity structures can be defined as a discontinuous set of components in compression within a continuous network of tensile elements. This definition is synthetized by the well-known expression: "island of compression in an ocean of tension" [7]. The overall performance of this kind of structures is strongly dependent on the way the different elementary cell are connected. Usually, the

*Corresponding author: gaetano.pavone@poliba.it
DOI: http://dxdoi.org/10.17515/resm2016.81st0727

structural analysis of these systems preliminarily requires a form-finding process [8-12], since their shape is strictly related to the self-stress in the elements. In this paper, a numerical study of the static response in the self-equilibrium state of a class of tensegrity grids, obtained by a suitable assembly of elementary V-Expander tensegrity cells along a longitudinal axis in three-dimensional space, is presented [13].

Notice that the analyzed V-Expander longitudinal grids form a sort of beam-like structures; hence, from now on, we refer to such structures with the term "beam". In particular, seven different "beams" made of V-Expander cells are analyzed. The aims of the paper are the following: 1) to identify the mechanical behavior of V-Expander tensegrity beams; 2) to evaluate the effects of the addition of elements into the structure on the feasible self-stress states.

In Section 2, we describe the form-finding problem for tensegrity structures: starting from some classic basic assumptions, we briefly recall how the self-equilibrium state can be determined. In Section 3, we define the parametric description of the geometry of the systems and the topology of the examined seven tensegrity structures. In Section 4, we discuss the obtained results and we show how the initial force vectors in the self-equilibrium state change as the geometric parameters vary.

2. Form-Finding for Tensegrity Structures

2.1. Basic assumptions

In the present study, we assume that:

- Elements are rectilinear and connected by pin joints.
- The connection between the struts is possible only at their extremities.
- Topology, i.e., the connectivity between nodes and elements, and the geometrical configuration in terms of nodal coordinates, are known.
- Self-weight of the elements is neglected, and no external loads are considered.
- Global and local buckling are not considered.
- The structure is free-standing (no supports are needed).

By virtue of these assumptions, only axial forces are carried by the elements, i.e., there are only two types of elements: struts in compression and cables in tension. A tensegrity structures is a system which possesses a stable self-equilibrated state. The latter is the initial mechanical state of the structure before any load, even gravitational, is applied. Furthermore, if a tensegrity structure possesses any infinitesimal mechanisms, these mechanisms are stabilized by the self-stress state in the elements; here, for the stability of the structure we mean the ability of the system to return to the equilibrium configuration after a small perturbation [14, 15].

2.2. Geometry and topology

In the three-dimensional space, a tensegrity structure has e elements: c cables and s struts (therefore, $c+s=e$); these elements are jointed at n nodes. In cable-net structures, apparently similar to the tensegrity structures, there are some fixed nodes due to the fact that only tension is carried by the cables [16]. From the above assumptions, tensegrity structures are free-standing, and therefore there exist only free nodes.

In order to define the geometrical configuration of a tensegrity structure, let **x**, **y** and **z** ($\in\mathbb{R}^n$) denote the nodal coordinate vectors of the free nodes in the directions $\mathbf{e}_x$, $\mathbf{e}_y$, $\mathbf{e}_z$ ($\in\mathbb{R}^3$)of an orthogonal reference system $O\{\mathbf{e}_x, \mathbf{e}_y, \mathbf{e}_z\}$.

The topology of the tensegrity structure can be assigned by using the well-known *connectivity matrix* $\mathbf{C}\in\mathbb{R}^{exn}$, which can be obtained as follows: suppose that the member k connects nodes i and j, with $i < j$; then, in the k-th row of **C** we have 1 and -1 at the i-th and j-th position, respectively:

$$[\mathbf{C}]_{k,p} = \begin{cases} 1 & \text{if } p = i \\ -1 & \text{if } p = j \\ 0 & \text{otherwise} \end{cases} . \tag{1}$$

It is helpful to define the vectors **u**, **v** and **w** ($\in\mathbb{R}^e$) of the coordinate differences of the elements in the x, y, z directions, respectively:

$$\begin{cases} \mathbf{u} = \mathbf{C}\mathbf{x} \\ \mathbf{v} = \mathbf{C}\mathbf{y} \\ \mathbf{w} = \mathbf{C}\mathbf{z} \end{cases}, \tag{2}$$

which collect the coordinate differences, u_k , v_k , and w_k, of the nodes corresponding to the ends of the k-th element (k = 1,..., e), connecting nodes i and j.

Furthermore, we define the vector $\mathbf{l}\in\mathbb{R}^e$ which is composed of the lengths of the elements. Let **U**, **V**, **W** and **L** ($\in\mathbb{R}^{exe}$) be the diagonal form of **u**, **v**, **w** and, **l** respectively, i.e., the diagonal matrices whose principal diagonals correspond to the above-mentioned vectors. Clearly, the diagonal matrix **L** can be expressed as:

$$\mathbf{L}^2 = \mathbf{U}^2 + \mathbf{V}^2 + \mathbf{W}^2. \tag{3}$$

This way, the geometrical configuration and the topology of the tensegrity structure are completely defined.

2.3. Self-equilibrium state

Once defined the geometrical configuration and the topology of a tensegrity structure, the equilibrium equations in each directions can be set as developed by Scheck [17]. In particular, the equilibrium equations, nonlinear in the unknown coordinates of the nodes, can be transformed in a set of linear equations by introducing the so-called force density q_k of the k-th element, that is the internal axial force to the length ratio [18]. Note that $q_k > 0$ for cables and $q_k < 0$ for struts. This condition is related to the unilateral mechanical behaviour of the elements, i.e., cables are in tension, and struts are in compression.

In absence of external loads, the self-equilibrium equations for a general free-standing pin-jointed structure can be written as [17]:

$$\begin{cases} \mathbf{C}^T\mathbf{Q}\mathbf{C}\mathbf{x} = \mathbf{0} \\ \mathbf{C}^T\mathbf{Q}\mathbf{C}\mathbf{y} = \mathbf{0} \\ \mathbf{C}^T\mathbf{Q}\mathbf{C}\mathbf{z} = \mathbf{0} \end{cases}, \tag{4}$$

where $\mathbf{Q}\in\mathbb{R}^{exe}$ is the diagonal matrix collecting the force densities of the elements. By introducing the *force density matrix* $\mathbf{D}\in\mathbb{R}^{nxn}$ as:

$$\mathbf{D} = \mathbf{C}^T\mathbf{Q}\mathbf{C}, \tag{5}$$

the equilibrium equations (4) can be rewritten as:

$$\begin{cases} \mathbf{Dx} = \mathbf{0} \\ \mathbf{Dy} = \mathbf{0}. \\ \mathbf{Dz} = \mathbf{0} \end{cases} \tag{6}$$

By observing that $diag(\mathbf{b})\mathbf{f}=diag(\mathbf{f})\mathbf{b}$, where **b** and **f** are generic vectors, and by introducing the so called *equilibrium matrix* $\mathbf{A}\in\mathbb{R}^{3nxe}$, (4) can be given as:

$$\begin{bmatrix} \mathbf{C}^T diag(\mathbf{Cx}) \\ \mathbf{C}^T diag(\mathbf{Cy}) \\ \mathbf{C}^T diag(\mathbf{Cz}) \end{bmatrix} \mathbf{q} = \mathbf{0}, \tag{7}$$

where the equilibrium matrix **A** is defined as:

$$\mathbf{A} = \begin{bmatrix} \mathbf{C}^T diag(\mathbf{Cx}) \\ \mathbf{C}^T diag(\mathbf{Cy}) \\ \mathbf{C}^T diag(\mathbf{Cz}) \end{bmatrix}. \tag{8}$$

From (7), the unknown basis of the vector space of the force densities of the elements lie in the null space of the equilibrium matrix **A**.

Let r_A and $\bar{r}_A$ be the rank and the dimension of the null space of the equilibrium matrix **A**, respectively. Then, there exist $\bar{r}_A$ *independent self-stress states* satisfying (7), that is:

$$\bar{r}_A = e - r_A. \tag{9}$$

Usually, tensegrity structures are statically indeterminate, and therefore there exist $\bar{r}_A$ ($\bar{r}_A \geq 1$) independent self-stress states, and each linear combination $\tilde{\mathbf{q}}_o\in\mathbb{R}^e$ of these vectors:

$$\tilde{\mathbf{q}}_o = \lambda_1 \mathbf{q}_1 + \ldots + \lambda_i \mathbf{q}_i + \ldots + \lambda_{\bar{r}_A} \mathbf{q}_{\bar{r}_A}, \tag{10}$$

where λ_i (i=1,2,..., $\bar{r}_A$) are real coefficients, is an independent self-stress state.

In general, the above vectors cannot be consistent with the unilateral behavior of the elements (struts in compression and cable in tension). In order to obtain independent self-stress states consistent with the unilateral behavior of the elements, the following procedure can be adopted.

If the structure has some symmetry properties, then elements in symmetric positions have the same force density, and they can be collected in a group. Let h, the number of the groups of symmetry which can be identified in the tensegrity structure; a vector $\tilde{\mathbf{q}}_i\in\mathbb{R}^e$ of independent self-stress states taking into account also the symmetry properties of the structure can be written as:

$$\tilde{\mathbf{q}}_i = \mathbf{e}_1 q_1 + \ldots + \mathbf{e}_i q_i + \ldots + \mathbf{e}_h q_h, \tag{11}$$

where the i-th component of the vector $\mathbf{e}_i\in\mathbb{R}^e$ (i=1,2,..., h) is equal to 1 if the related element belongs to the i-th group of symmetry, and it is equal to 0 otherwise, and q_i (i=1,2,..., h) is the force density of the elements of the i-th group of symmetry. The independent self-stress states (11), consistent with the symmetry of the structure, are called *integral self-stress states*. Moreover, a *feasible self-stress state* $\tilde{\mathbf{q}}_a\in\mathbb{R}^e$ is defined as an integral self-stress state consistent also with the unilateral behaviour of the elements.

In [19] it is presented a numerical method for initial self-stress design of tensegrity structures which leads to feasible self-stress states; here, we briefly recall the main steps of this algorithm. From (10) and (11), it is possible to write:

$$\lambda_1\mathbf{q}_1+\ldots+\lambda_i\mathbf{q}_i+\ldots+\lambda_{\bar{r}_A}\mathbf{q}_{\bar{r}_A}-\left(\mathbf{e}_1q_1+\ldots+\mathbf{e}_iq_i+\ldots+\mathbf{e}_hq_h\right)=\mathbf{0}. \tag{12}$$

We can introduce the matrix $\mathbf{G}\in\mathbb{R}^{ex(\bar{r}_A+h)}$ whose first $\bar{r}_A$ columns are the vectors $\mathbf{q}_i$ (i=1,2,..., $\bar{r}_A$) and the last h columns are the vectors -$\mathbf{e}_i$ (i=1,2,..., h), and the vector $\bar{\boldsymbol{\beta}}\in\mathbb{R}^{(\bar{r}_A+h)}$ whose first $\bar{r}_A$ components are the real coefficients λ_i (i=1,2,..., $\bar{r}_A$) in (10) and the last h elements are the force density q_i (i=1,2,..., h) of the elements of each group:

$$\mathbf{G}=\left[\mathbf{q}_1,\ldots,\mathbf{q}_i,\ldots,\mathbf{q}_{\bar{r}_A},-\mathbf{e}_1,\ldots,-\mathbf{e}_i,\ldots,-\mathbf{e}_h\right], \tag{13}$$

$$\bar{\boldsymbol{\beta}}=\left[\lambda_1,\ldots,\lambda_i,\ldots+\lambda_{\bar{r}_A},q_1,\ldots,q_i,\ldots,q_h\right]. \tag{14}$$

By (13)-(14), (12) can be rewritten as:

$$\mathbf{G}\bar{\boldsymbol{\beta}}=\mathbf{0}. \tag{15}$$

A Singular Value Decomposition (SVD) should be carried out [20] in order to find all the solutions of (15), which lie in the null space of **G**. In this vein, it is important to notice that the dimension of the null space and the rank of **G** are equal to $\bar{r}_G$ and $\bar{r}_G$, respectively. Thus, we have:

$$\bar{r}_G=\left(\bar{r}_A+h\right)-r_G. \tag{16}$$

If the dimension of the null space of **G** is equal to 1, the tensegrity structure has only one integral self-stress mode $\tilde{\mathbf{q}}_i$. If the force densities of the elements are consistent with the unilateral behaviour of the cables and struts, then this integral self-stress mode also corresponds to a feasible self-stress mode $\tilde{\mathbf{q}}_a$.

If the dimension of the null space of **G** is equal to zero, (15) has only trivial solutions. In this case, the tensegrity structure cannot be in an integral self-stress state consistent with the considered geometric symmetry. However, it is possible to vary $\bar{r}_G$ by suitably increasing the number of the groups of the symmetry until $\bar{r}_G$ become equal to 1.

Finally, if $\bar{r}_G > 1$, i.e., (15) has multiple solutions, there exist more than one integral self-stress modes. Now, in order to have $\bar{r}_G$ equal to 1, the number of the groups should be decreased. Alternatively, a linear combination of these $\bar{r}_G$ vectors is still a solution of (15), which, generally, is not consistent with the unilateral rigidities of the elements. Anyway, by solving an optimization problem in multiple variables [21], for example, it is possible to find feasible self-stress states as a suitable linear combination of the $\bar{r}_G$ integral self-stress modes.

After determining a feasible self-stress state, we can find the initial force vector in the self-equilibrium state, $\bar{\mathbf{f}}_i\in\mathbb{R}^e$:

$$\bar{\mathbf{f}}_i=\mathbf{L}\bar{\mathbf{q}}_a. \tag{17}$$

2.4. Infinitesimal mechanisms

Let $\boldsymbol{\varepsilon}\in\mathbb{R}^e$, and $\mathbf{d}\in\mathbb{R}^{3n}$ the vectors of the axial strain of the elements and the vector of the nodal displacements, respectively. By the principle of virtual works:

$$\mathbf{A}^T\mathbf{d}=\boldsymbol{\varepsilon}. \tag{18}$$

Infinitesimal mechanisms $\mathbf{d}_m \in \mathbb{R}^{3n}$ are vectors of nodal displacements which correspond to zero axial strains:

$$\mathbf{A}^T \mathbf{d}_m = \mathbf{0}. \tag{19}$$

By (19), infinitesimal mechanisms lie in the null space of the transpose of the equilibrium matrix **A**. Since we consider free-standing structures, this null space also contains six rigid-body motions in the three-dimensional space. Thus, the multiplicity of the infinitesimal mechanisms $\bar{r}_{A^T}$, is:

$$\bar{r}_{A^T} = 3n - r_A - 6. \tag{20}$$

2.5. Rank deficiency conditions

Let r_D the rank of the force density matrix; then, the dimension of the null space of **D** is

$$\bar{r}_D = n - r_D. \tag{21}$$

Hence, in order to create a space of solution of (6) having at least four dimensions, the dimension of the null space of **D** should be equal or greater than four. Furthermore, we recall that the dimension of the null space of the equilibrium matrix **A** should be equal or greater than one.

3. V-Expander Tensegrity Beam-Like Grids

In this work, we focalize our attention on the elementary tensegrity cell called V-Expander. The first realization of a tensegrity structure based on this concept is the Tensegrity mast built by Buckminster Fuller, S. Sadao and E. Price in 1959. In 2002, R. Motro and V. Raducanu patented this tensegrity cell within the activities of the research project "*Tensarch Project*" [22].

A V-Expander tensegrity cell is composed by four struts and nine cables, which are joined by six nodes (Fig. 1). Two couples of struts form two orthogonal triangles in the three-dimensional space. The vertical cable represents the intersection of these two triangles, and it materializes the *expander axis* of the cell: by reducing its length, it is possible to introduce a self-stress in all the elements of the structure.

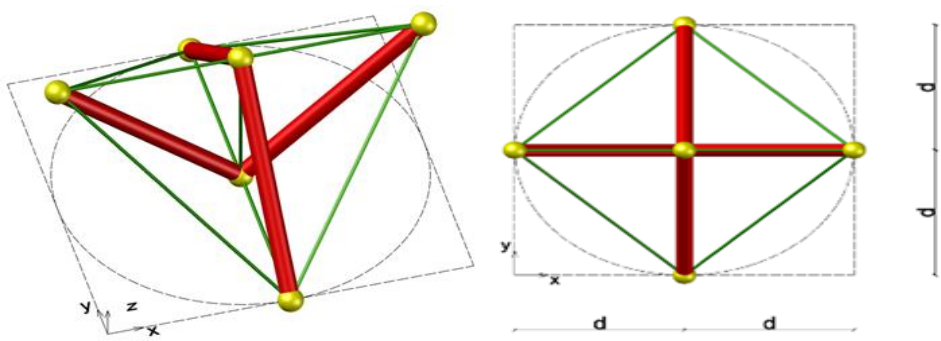

Fig. 1 Perspective view and top view of V_{22}-Expander tensegrity cell

Usually, a V-Expander tensegrity cell is denoted as V_{mn}, where the subscripts *m* and *n* are the number of the struts connected at the lower node and at the upper node of the expander axis, respectively. For issues related to the symmetry of the cell, it is better to have *m*=*n*.

Generally, a tensegrity structure that has no contacts between its struts is named class 1 tensegrity system, and tensegrity system with as many as *k* struts in contact is named class *k* tensegrity system [23, 24] (for *k* tensegrity systems the discontinuous set of components in compression can be obtained by an arrangement of elements [25-28]). Thus, V-Expander tensegrity cells belong to class 2 tensegrity systems, i.e., tensegrity structures with as many as 2 struts in contact at their extremities.

By composing V-Expander tensegrity elementary cells, it is possible to build, with great simplicity, bi-, and tri-directional tensegrity grids (or towers, arches, etc.). In all those complex systems, self-stress states can be still introduced only acting on the length of some vertical cables [29, 30].

In this paper, we analyze a V-Expander Tensegrity beams obtained by assembling three V_{22}-Expander tensegrity cells along a direction called *x*-axis in the considered orthogonal reference system $O\{\mathbf{e}_x, \mathbf{e}_y, \mathbf{e}_z\}$. In particular, we study seven V-expander tensegrity structures with increasing complexity:

- *Case 1*, 43 elements.
- *Case 2*, 53 elements.
- *Case 3*, 57 elements.
- *Case 4*, 59 elements.
- *Case 5*, 63 elements.
- *Case 6*, 67 elements.
- *Case 7*, 71 elements.

In particular, we analyze the feasible self-stress state $\tilde{\mathbf{q}}_a$ of the above-mentioned seven structures.

First, we consider a V-Expander beam (*Case 1*) composed of 16 struts and 27 cables; 22 nodes connect the elements of the grid (nodes and elements are labelled in view of geometrical symmetry of the structure, see Fig. 2).

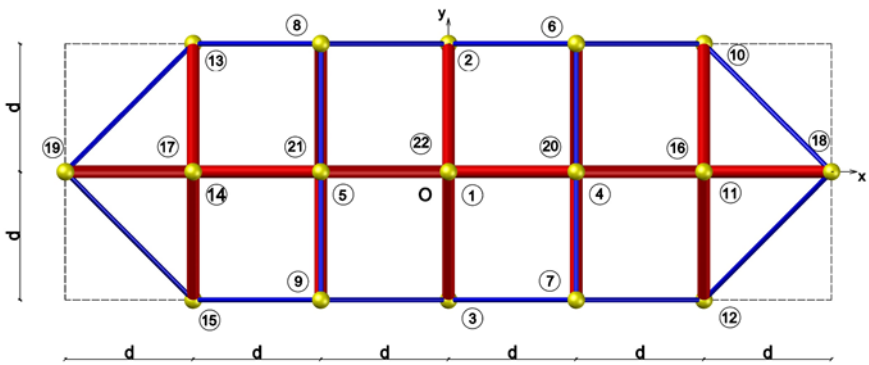

Fig. 2 Top view of Case 1

In all the above-mentioned seven cases, the grid is enclosed by a parallelepiped, whose lengths of edges are 6*d*, 2*d* and *h*, in *x*, *y* and *z* direction respectively. For the sake of clarity, labels on the top-left of the nodes represent the top layer of the grid ($z = h$), and labels on bottom-right indicate the lower level of the structure ($z = 0$).

Specifically, *Case 1*, is composed of the following elements (Fig. 3):

- 27 cables (*1*, *2*, *5*, *8*, *9*, *10*, *11*, *12*, *13*, *18*, *19*, *20*, *21*, *22*, *23*, *30*, *31*, *32*, *33*, *34*, *35*, *36*, *37*, *38*, *39*, *40*, *41*) and 16 struts (from *48* to *63*).

By (1), for Case 1 we have the following connectivity matrix $\mathbf{C}\in\mathbb{R}^{43x22}$ (the labels of the elements are shown in the right-hand list):

$$
\left[\begin{array}{cccccccccccccccccccccc}
1 & -1 & 0 & 0 & 0 & 0 & 0 & 0 & 0 & 0 & 0 & 0 & 0 & 0 & 0 & 0 & 0 & 0 & 0 & 0 & 0 & 0 \\
1 & 0 & -1 & 0 & 0 & 0 & 0 & 0 & 0 & 0 & 0 & 0 & 0 & 0 & 0 & 0 & 0 & 0 & 0 & 0 & 0 & 0 \\
1 & 0 & 0 & 0 & 0 & 0 & 0 & 0 & 0 & 0 & 0 & 0 & 0 & 0 & 0 & 0 & 0 & 0 & 0 & 0 & 0 & -1 \\
0 & 0 & 0 & 0 & 0 & 1 & 0 & 0 & 0 & 0 & 0 & 0 & 0 & 0 & 0 & 0 & 0 & 0 & 0 & -1 & 0 & 0 \\
0 & 0 & 0 & 0 & 0 & 0 & 1 & 0 & 0 & 0 & 0 & 0 & 0 & 0 & 0 & 0 & 0 & 0 & 0 & -1 & 0 & 0 \\
0 & 0 & 0 & 0 & 0 & 0 & 0 & 1 & 0 & 0 & 0 & 0 & 0 & 0 & 0 & 0 & 0 & 0 & 0 & 0 & -1 & 0 \\
0 & 0 & 0 & 0 & 0 & 0 & 0 & 0 & 1 & 0 & 0 & 0 & 0 & 0 & 0 & 0 & 0 & 0 & 0 & 0 & -1 & 0 \\
0 & 0 & 0 & 1 & 0 & 0 & 0 & 0 & 0 & 0 & 0 & 0 & 0 & 0 & 0 & 0 & 0 & 0 & 0 & -1 & 0 & 0 \\
0 & 0 & 0 & 0 & 1 & 0 & 0 & 0 & 0 & 0 & 0 & 0 & 0 & 0 & 0 & 0 & 0 & 0 & 0 & 0 & -1 & 0 \\
0 & 0 & 0 & 0 & 0 & 0 & 0 & 0 & 0 & 1 & -1 & 0 & 0 & 0 & 0 & 0 & 0 & 0 & 0 & 0 & 0 & 0 \\
0 & 0 & 0 & 0 & 0 & 0 & 0 & 0 & 0 & 0 & 1 & -1 & 0 & 0 & 0 & 0 & 0 & 0 & 0 & 0 & 0 & 0 \\
0 & 0 & 0 & 0 & 0 & 0 & 0 & 0 & 0 & 0 & 0 & 0 & 1 & -1 & 0 & 0 & 0 & 0 & 0 & 0 & 0 & 0 \\
0 & 0 & 0 & 0 & 0 & 0 & 0 & 0 & 0 & 0 & 0 & 0 & 0 & 1 & -1 & 0 & 0 & 0 & 0 & 0 & 0 & 0 \\
0 & 0 & 0 & 0 & 0 & 0 & 0 & 0 & 0 & 0 & 1 & 0 & 0 & 0 & 0 & -1 & 0 & 0 & 0 & 0 & 0 & 0 \\
0 & 0 & 0 & 0 & 0 & 0 & 0 & 0 & 0 & 0 & 0 & 0 & 0 & 1 & 0 & 0 & -1 & 0 & 0 & 0 & 0 & 0 \\
0 & 0 & 0 & 0 & 0 & 0 & 0 & 0 & 0 & 1 & 0 & 0 & 0 & 0 & 0 & 0 & 0 & -1 & 0 & 0 & 0 & 0 \\
0 & 0 & 0 & 0 & 0 & 0 & 0 & 0 & 0 & 0 & 0 & 0 & 1 & 0 & 0 & 0 & 0 & 0 & -1 & 0 & 0 & 0 \\
0 & 0 & 0 & 0 & 0 & 0 & 0 & 0 & 0 & 0 & 0 & 0 & 0 & 1 & 0 & 0 & 0 & 0 & 0 & -1 & 0 & 0 \\
0 & 0 & 0 & 0 & 0 & 1 & 0 & 0 & 0 & -1 & 0 & 0 & 0 & 0 & 0 & 0 & 0 & 0 & 0 & 0 & 0 & 0 \\
0 & 0 & 0 & 0 & 0 & 0 & 1 & 0 & 0 & 0 & 0 & -1 & 0 & 0 & 0 & 0 & 0 & 0 & 0 & 0 & 0 & 0 \\
0 & 0 & 0 & 0 & 0 & 0 & 0 & 1 & 0 & 0 & 0 & 0 & -1 & 0 & 0 & 0 & 0 & 0 & 0 & 0 & 0 & 0 \\
0 & 0 & 0 & 0 & 0 & 0 & 0 & 0 & 1 & 0 & 0 & 0 & 0 & 0 & -1 & 0 & 0 & 0 & 0 & 0 & 0 & 0 \\
0 & 1 & 0 & 0 & 0 & -1 & 0 & 0 & 0 & 0 & 0 & 0 & 0 & 0 & 0 & 0 & 0 & 0 & 0 & 0 & 0 & 0 \\
0 & 0 & 1 & 0 & 0 & 0 & -1 & 0 & 0 & 0 & 0 & 0 & 0 & 0 & 0 & 0 & 0 & 0 & 0 & 0 & 0 & 0 \\
0 & 1 & 0 & 0 & 0 & 0 & 0 & -1 & 0 & 0 & 0 & 0 & 0 & 0 & 0 & 0 & 0 & 0 & 0 & 0 & 0 & 0 \\
0 & 0 & 1 & 0 & 0 & 0 & 0 & 0 & -1 & 0 & 0 & 0 & 0 & 0 & 0 & 0 & 0 & 0 & 0 & 0 & 0 & 0 \\
0 & 1 & 0 & 0 & 0 & 0 & 0 & 0 & 0 & 0 & 0 & 0 & 0 & 0 & 0 & 0 & 0 & 0 & 0 & 0 & 0 & -1 \\
0 & 0 & 1 & 0 & 0 & 0 & 0 & 0 & 0 & 0 & 0 & 0 & 0 & 0 & 0 & 0 & 0 & 0 & 0 & 0 & 0 & -1 \\
1 & 0 & 0 & 0 & 0 & 0 & 0 & 0 & 0 & 0 & 0 & 0 & 0 & 0 & 0 & 0 & 0 & 0 & 0 & -1 & 0 & 0 \\
1 & 0 & 0 & 0 & 0 & 0 & 0 & 0 & 0 & 0 & 0 & 0 & 0 & 0 & 0 & 0 & 0 & 0 & 0 & 0 & -1 & 0 \\
0 & 0 & 0 & 1 & 0 & -1 & 0 & 0 & 0 & 0 & 0 & 0 & 0 & 0 & 0 & 0 & 0 & 0 & 0 & 0 & 0 & 0 \\
0 & 0 & 0 & 1 & 0 & 0 & -1 & 0 & 0 & 0 & 0 & 0 & 0 & 0 & 0 & 0 & 0 & 0 & 0 & 0 & 0 & 0 \\
0 & 0 & 0 & 0 & 1 & 0 & 0 & -1 & 0 & 0 & 0 & 0 & 0 & 0 & 0 & 0 & 0 & 0 & 0 & 0 & 0 & 0 \\
0 & 0 & 0 & 0 & 1 & 0 & 0 & 0 & -1 & 0 & 0 & 0 & 0 & 0 & 0 & 0 & 0 & 0 & 0 & 0 & 0 & 0 \\
0 & 0 & 0 & 0 & 0 & 0 & 0 & 0 & 0 & 0 & 1 & 0 & 0 & 0 & 0 & 0 & 0 & 0 & 0 & -1 & 0 & 0 \\
0 & 0 & 0 & 0 & 0 & 0 & 0 & 0 & 0 & 0 & 0 & 0 & 0 & 1 & 0 & 0 & 0 & 0 & 0 & 0 & -1 & 0 \\
0 & 0 & 0 & 0 & 0 & 0 & 0 & 0 & 0 & 1 & 0 & 0 & 0 & 0 & 0 & -1 & 0 & 0 & 0 & 0 & 0 & 0 \\
0 & 0 & 0 & 0 & 0 & 0 & 0 & 0 & 0 & 0 & 0 & 0 & 1 & 0 & 0 & 0 & -1 & 0 & 0 & 0 & 0 & 0 \\
0 & 0 & 0 & 0 & 0 & 0 & 0 & 0 & 0 & 0 & 0 & 0 & 0 & 1 & 0 & -1 & 0 & 0 & 0 & 0 & 0 & 0 \\
0 & 0 & 0 & 0 & 0 & 0 & 0 & 0 & 0 & 0 & 1 & 0 & 0 & 0 & 0 & 0 & -1 & 0 & 0 & 0 & 0 & 0 \\
0 & 0 & 0 & 0 & 0 & 0 & 0 & 0 & 0 & 0 & 0 & 0 & 0 & 1 & 0 & 0 & 0 & 0 & -1 & 0 & 0 & 0
\end{array}\right]
\begin{array}{c}
1 \\ 2 \\ 5 \\ 8 \\ 9 \\ 10 \\ 11 \\ 12 \\ 13 \\ 18 \\ 19 \\ 20 \\ 21 \\ 22 \\ 23 \\ 30 \\ 31 \\ 32 \\ 33 \\ 34 \\ 35 \\ 36 \\ 37 \\ 38 \\ 39 \\ 40 \\ 41 \\ 48 \\ 49 \\ 50 \\ 51 \\ 52 \\ 53 \\ 54 \\ 55 \\ 56 \\ 57 \\ 58 \\ 59 \\ 60 \\ 61 \\ 62 \\ 63
\end{array}
\tag{22}
$$

The other cases are obtained, starting form *Case 1*, by addition of elements (insertion respects geometrical symmetry of the structure) as follow:

- *Case 2*, 10 elements (*3*, *4*, *6*, *7*, *24*, *25*, *26*, *27*, *28*, *29*) added to *Case 1*, see Fig. 4.

$$
\left[\begin{array}{cccccccccccccccccccccc}
1 & 0 & 0 & 0 & -1 & 0 & 0 & 0 & 0 & 0 & 0 & 0 & 0 & 0 & 0 & 0 & 0 & 0 & 0 & 0 & 0 & 0 \\
1 & 0 & 0 & -1 & 0 & 0 & 0 & 0 & 0 & 0 & 0 & 0 & 0 & 0 & 0 & 0 & 0 & 0 & 0 & 0 & 0 & 0 \\
 & & & & & & & & & & & \vdots & & & & & & & & & & \\
0 & 0 & 0 & 0 & 0 & 0 & 0 & 0 & 0 & 0 & 0 & 0 & 0 & 0 & 0 & 0 & 0 & 0 & 0 & 0 & 1 & -1 \\
0 & 0 & 0 & 0 & 0 & 0 & 0 & 0 & 0 & 0 & 0 & 0 & 0 & 0 & 0 & 0 & 0 & 0 & 0 & 1 & 0 & -1 \\
 & & & & & & & & & & & \vdots & & & & & & & & & & \\
0 & 0 & 0 & 0 & 0 & 0 & 0 & 0 & 0 & 0 & 0 & 0 & 0 & 0 & 0 & 1 & 0 & -1 & 0 & 0 & 0 & 0 \\
0 & 0 & 0 & 0 & 0 & 0 & 0 & 0 & 0 & 0 & 0 & 0 & 0 & 0 & 0 & 0 & 1 & 0 & -1 & 0 & 0 & 0 \\
0 & 0 & 0 & 0 & 0 & 1 & 0 & 0 & 0 & 0 & 0 & 0 & 0 & 0 & 0 & 0 & 0 & 0 & -1 & 0 & 0 & 0 \\
0 & 0 & 0 & 0 & 0 & 0 & 1 & 0 & 0 & 0 & 0 & 0 & 0 & 0 & 0 & 0 & 0 & 0 & -1 & 0 & 0 & 0 \\
0 & 0 & 0 & 0 & 0 & 0 & 0 & 1 & 0 & 0 & 0 & 0 & 0 & 0 & 0 & 0 & 0 & 0 & 0 & -1 & 0 & 0 \\
0 & 0 & 0 & 0 & 0 & 0 & 0 & 0 & 1 & 0 & 0 & 0 & 0 & 0 & 0 & 0 & 0 & 0 & 0 & -1 & 0 & 0
\end{array}\right]
\begin{array}{c}
3 \\ 4 \\ \vdots \\ 6 \\ 7 \\ \vdots \\ 24 \\ 25 \\ 26 \\ 27 \\ 28 \\ 29
\end{array}
\tag{23}
$$

- *Case 3*, 4 elements (*14*, *15*, *16*, *17*) added to *Case 2*, see Fig. 5.

$$\begin{array}{c} \vdots \\ \left[\begin{array}{cccccccccccccccccccccc} & & & & & & & & & & & \vdots & & & & & & & & & & \\ 0 & 0 & 0 & 1 & 0 & 0 & 0 & 0 & 0 & 0 & -1 & 0 & 0 & 0 & 0 & 0 & 0 & 0 & 0 & 0 & 0 & 0 \\ 0 & 0 & 0 & 0 & 1 & 0 & 0 & 0 & 0 & 0 & 0 & 0 & 0 & -1 & 0 & 0 & 0 & 0 & 0 & 0 & 0 & 0 \\ 0 & 0 & 0 & 0 & 0 & 0 & 0 & 0 & 0 & 0 & 0 & 0 & 0 & 0 & 0 & 1 & 0 & 0 & 0 & -1 & 0 & 0 \\ 0 & 0 & 0 & 0 & 0 & 0 & 0 & 0 & 0 & 0 & 0 & 0 & 0 & 0 & 0 & 0 & 1 & 0 & 0 & 0 & -1 & 0 \\ & & & & & & & & & & & \vdots & & & & & & & & & & \end{array}\right] \end{array} \begin{array}{c} \vdots \\ 14 \\ 15 \\ 16 \\ 17 \\ \vdots \end{array} \tag{24}$$

- *Case 4*, 2 elements (*42*, *43*) added to *Case 3*, see Fig. 6.

$$\begin{array}{c} \vdots \\ \left[\begin{array}{cccccccccccccccccccccc} & & & & & & & & & & & \vdots & & & & & & & & & & \\ 0 & 0 & 0 & 0 & 0 & 1 & 0 & -1 & 0 & 0 & 0 & 0 & 0 & 0 & 0 & 0 & 0 & 0 & 0 & 0 & 0 & 0 \\ 0 & 0 & 0 & 0 & 0 & 0 & 1 & 0 & -1 & 0 & 0 & 0 & 0 & 0 & 0 & 0 & 0 & 0 & 0 & 0 & 0 & 0 \\ & & & & & & & & & & & \vdots & & & & & & & & & & \end{array}\right] \end{array} \begin{array}{c} \vdots \\ 42 \\ 43 \\ \vdots \end{array} \tag{25}$$

- *Case 5*, 4 elements (*44*, *45*, *46*, *47*) added to *Case 4*, see Fig. 7.

$$\begin{array}{c} \vdots \\ \left[\begin{array}{cccccccccccccccccccccc} & & & & & & & & & & & \vdots & & & & & & & & & & \\ 0 & 1 & 0 & 0 & 0 & 0 & 0 & 0 & 0 & -1 & 0 & 0 & 0 & 0 & 0 & 0 & 0 & 0 & 0 & 0 & 0 & 0 \\ 0 & 0 & 1 & 0 & 0 & 0 & 0 & 0 & 0 & 0 & 0 & -1 & 0 & 0 & 0 & 0 & 0 & 0 & 0 & 0 & 0 & 0 \\ 0 & 1 & 0 & 0 & 0 & 0 & 0 & 0 & 0 & 0 & 0 & 0 & -1 & 0 & 0 & 0 & 0 & 0 & 0 & 0 & 0 & 0 \\ 0 & 0 & 1 & 0 & 0 & 0 & 0 & 0 & 0 & 0 & 0 & 0 & 0 & 0 & -1 & 0 & 0 & 0 & 0 & 0 & 0 & 0 \\ & & & & & & & & & & & \vdots & & & & & & & & & & \end{array}\right] \end{array} \begin{array}{c} \vdots \\ 44 \\ 45 \\ 46 \\ 47 \\ \vdots \end{array} \tag{26}$$

- *Case 6*, 4 elements (*64*, *65*, *66*, *67*) added to *Case 5*, see Fig. 8.

$$\begin{array}{c} \vdots \\ \left[\begin{array}{cccccccccccccccccccccc} & & & & & & & & & & & \vdots & & & & & & & & & & \\ 0 & 0 & 0 & 0 & 0 & 1 & 0 & 0 & 0 & 0 & 0 & 0 & 0 & 0 & 0 & 0 & 0 & 0 & 0 & 0 & 0 & -1 \\ 0 & 0 & 0 & 0 & 0 & 0 & 1 & 0 & 0 & 0 & 0 & 0 & 0 & 0 & 0 & 0 & 0 & 0 & 0 & 0 & 0 & -1 \\ 0 & 0 & 0 & 0 & 0 & 0 & 0 & 1 & 0 & 0 & 0 & 0 & 0 & 0 & 0 & 0 & 0 & 0 & 0 & 0 & 0 & -1 \\ 0 & 0 & 0 & 0 & 0 & 0 & 0 & 0 & 1 & 0 & 0 & 0 & 0 & 0 & 0 & 0 & 0 & 0 & 0 & 0 & 0 & -1 \end{array}\right] \end{array} \begin{array}{c} \vdots \\ 64 \\ 65 \\ 66 \\ 67 \end{array} \tag{27}$$

- *Case 7*, 4 elements (*68*, *69*, *70*, *71*) added to *Case 6*, see Fig. 9.

$$\begin{array}{c} \vdots \\ \left[\begin{array}{cccccccccccccccccccccc} & & & & & & & & & & & \vdots & & & & & & & & & & \\ 0 & 0 & 0 & 0 & 0 & 1 & 0 & 0 & 0 & 0 & 0 & 0 & 0 & 0 & 0 & -1 & 0 & 0 & 0 & 0 & 0 & 0 \\ 0 & 0 & 0 & 0 & 0 & 0 & 1 & 0 & 0 & 0 & 0 & 0 & 0 & 0 & 0 & -1 & 0 & 0 & 0 & 0 & 0 & 0 \\ 0 & 0 & 0 & 0 & 0 & 0 & 0 & 1 & 0 & 0 & 0 & 0 & 0 & 0 & 0 & 0 & -1 & 0 & 0 & 0 & 0 & 0 \\ 0 & 0 & 0 & 0 & 0 & 0 & 0 & 0 & 1 & 0 & 0 & 0 & 0 & 0 & 0 & 0 & -1 & 0 & 0 & 0 & 0 & 0 \end{array}\right] \end{array} \begin{array}{c} \vdots \\ 68 \\ 69 \\ 70 \\ 71 \end{array} \tag{28}$$

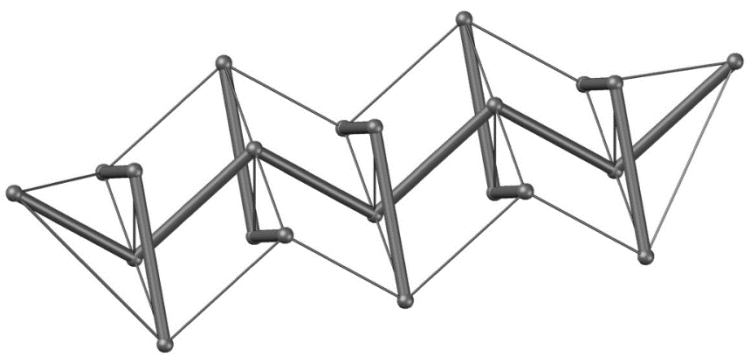

Fig. 3 Perspective view of *Case 1*

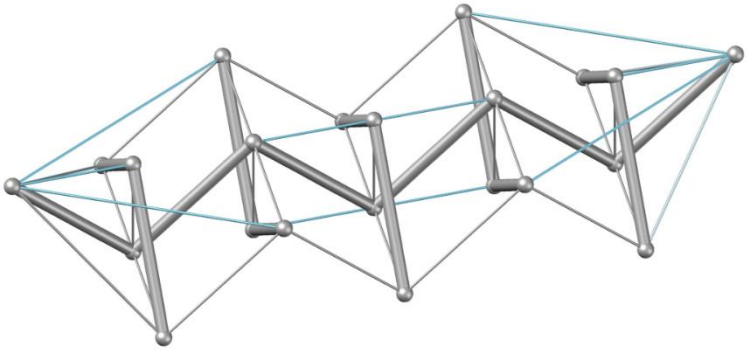

Fig. 4 Perspective view of *Case 2* (additional elements with respect to *Case 1* in pale-blue)

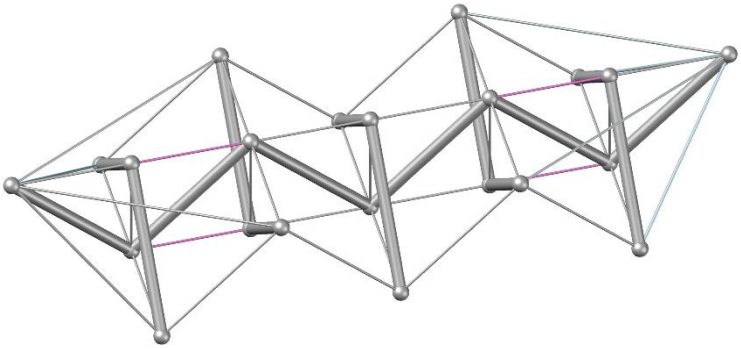

Fig. 5 Perspective view of *Case 3* (additional elements with respect to *Case 2* in purple)

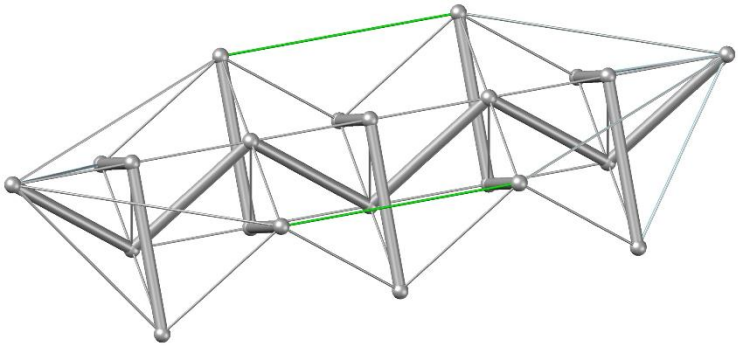

Fig. 6 Perspective view of *Case 4* (additional elements with respect to *Case 3* in green)

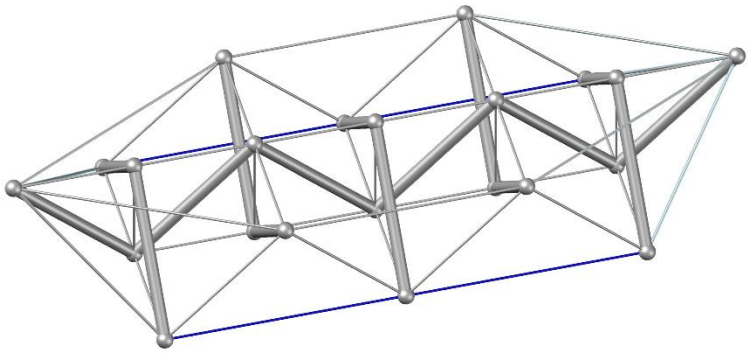

Fig. 7 Perspective view of *Case 5* (additional elements with respect to *Case 4* in light blue)

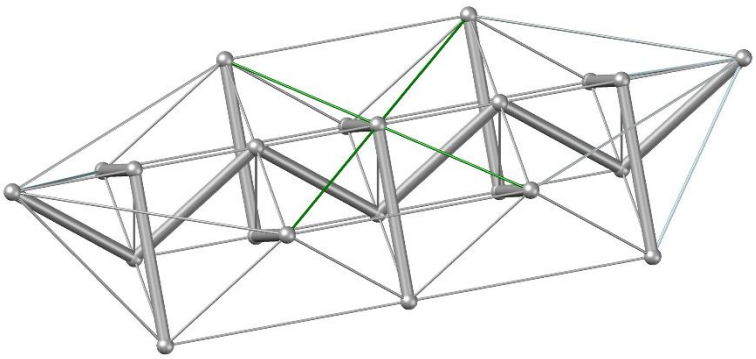

Fig. 8 Perspective view of *Case 6* (additional elements with respect to *Case5* in green)

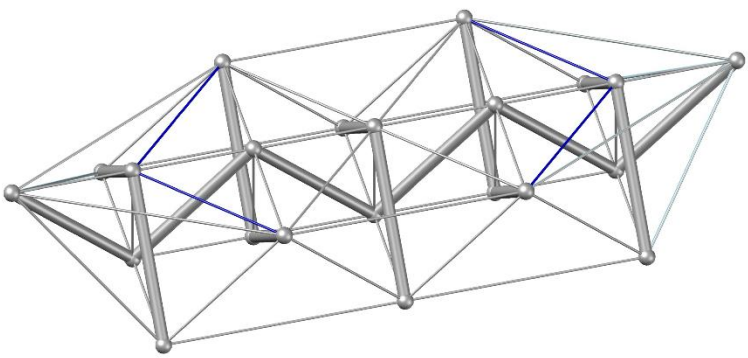

Fig. 9 Perspective view of *Case 7* (additional elements with respect to *Case 6* in dark blue)

4. Results and Discussion

As the number of the elements increases, the rank of the equilibrium matrix **A** increases and then the number of the independent self-stress states also increases. Simultaneously, the number of the infinitesimal mechanisms of the V-Expander tensegrity beams decreases.

In particular, *Case 1* possesses 18 infinitesimal mechanisms in addition to the 6 rigid-body motions in three-dimensional space. On the contrary, no infinitesimal mechanisms lie in the null space of the transpose of the equilibrium matrix **A** for *Case 7* when rigid-body motions are excluded, that is, *Case 7* is a kinematically determinate tensegrity structure. Fig. 10 shows the number of the independent self-stress states and the number of the infinitesimal mechanisms for every V-Expander tensegrity beams under investigation.

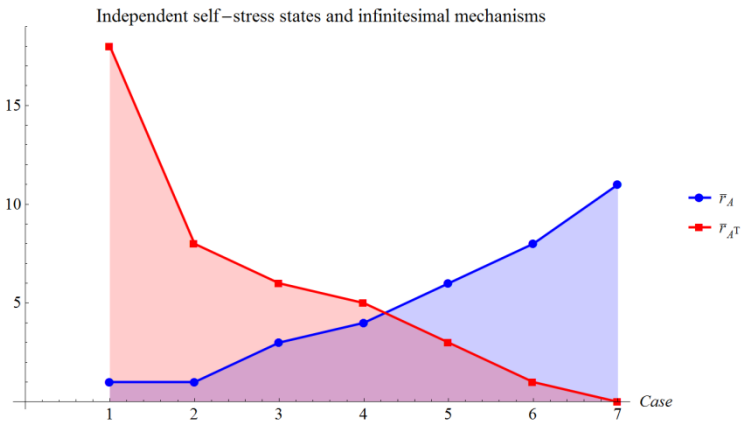

Fig. 10 Number of independent self-stress states *s* and number of infinitesimal mechanisms *m* of the seven V-Expander tensegrity beams.

In Table 1 are listed the properties of the seven V-Expander beams, i.e., the dimensions of the connectivity matrix **C** and the dimensions and the rank of the equilibrium matrix **A**.

Table 1. Properties of the seven V-Expander beams

Case		*1*	*2*	*3*	*4*	*5*	*6*	*7*
Properties of V-Expander beams	$\mathbf{C}\in\mathbb{R}^{exn}$	43 x 22	53 x 22	57 x 22	59 x 22	63 x 22	67 x 22	71 x 22
	$\mathbf{A}\in\mathbb{R}^{3nxe}$	66 x 43	66 x 53	66 x 57	66 x 59	66 x 63	66 x 67	66 x 71
	r_A	42	52	54	55	57	59	60

For *Case* 1, as well as for Case *2*, we have only one independent self-stress state $\mathbf{q}_1$, which is consistent with the symmetry properties of the structure and the unilateral behavior of the elements. Thus, this vector represents a feasible self-stress state $\tilde{\mathbf{q}}_a$.

For what concerns the other cases, there exist more than one independent self-stress states $\mathbf{q}_i$; therefore, feasible self-stress states can be obtained by following the procedure described in the Section 2.3.

In order to analyze the mechanical behavior of the seven V-Expander tensegrity beams in their self-equilibrium state, we calculate the initial force vector $\bar{\mathbf{f}}_i$ by (17). The parametric description of the geometry of the structures allow us to express the feasible self-stress state $\tilde{\mathbf{q}}_a$ as a function of the parameters *d* and *h*. In Figures 11-17 we plot for all tensegrity beams under investigation the initial force vectors, for *h*=1 and for values of the parameter *d* ranging from 0.01*h* (extremely compact grids) to *h* (square cell grids); the blue line represents the internal force in the elements for *d*=0.5*h*.

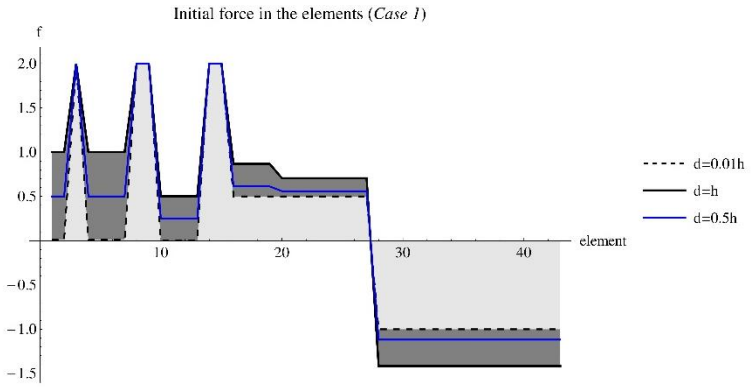

Fig. 11 Initial force vector; *Case 1* ($d \in [0.01h, h]$)

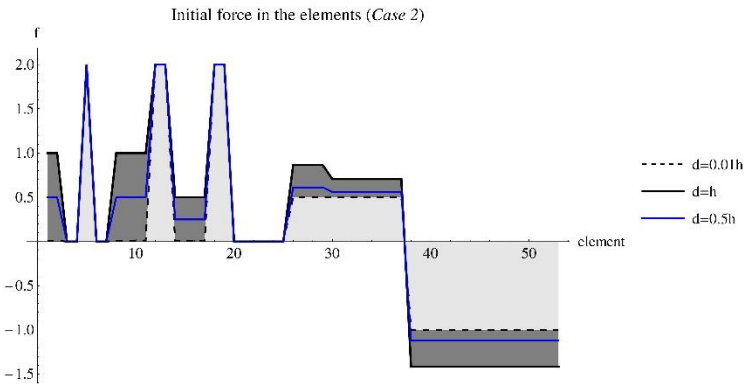

Fig. 12 Initial force vector; *Case 2* ($d \in [0.01h, h]$)

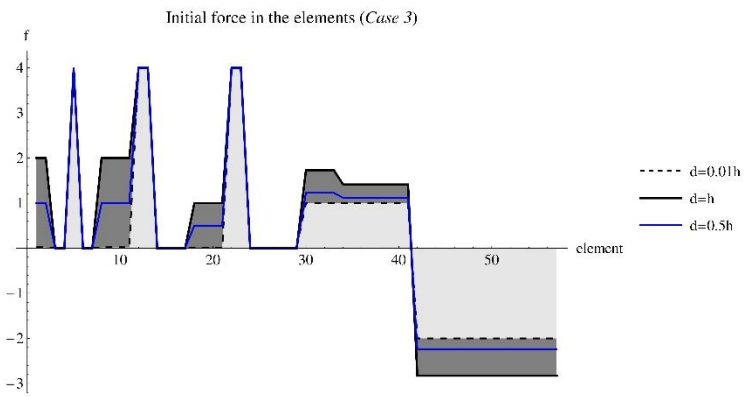

Fig. 13 Initial force vector; *Case 3* ($d \in [0.01h, h]$)

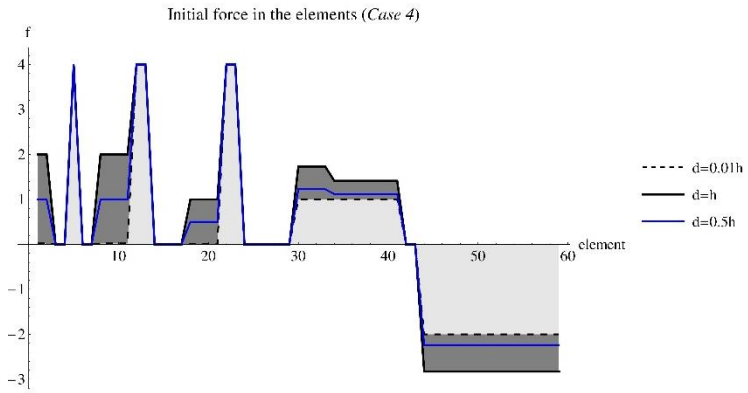

Fig. 14 Initial force vector; *Case 4* ($d \in [0.01h, h]$)

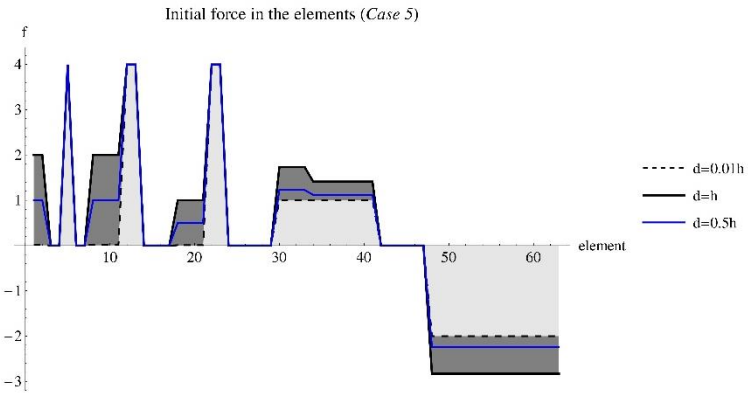

Fig. 15 Initial force vector; *Case 5* ($d \in [0.01h, h]$)

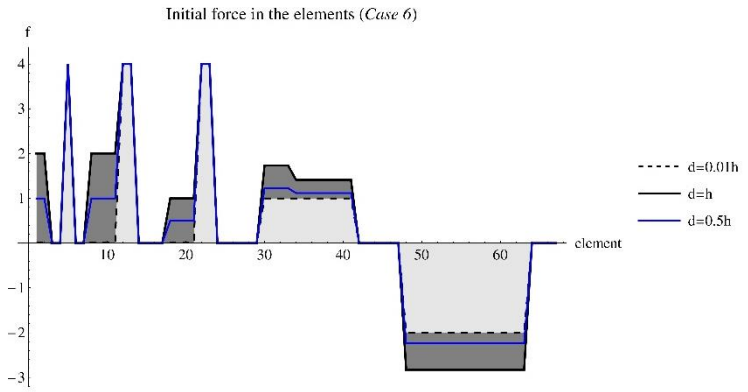

Fig. 16 Initial force vector; *Case 6* ($d \in [0.01h, h]$)

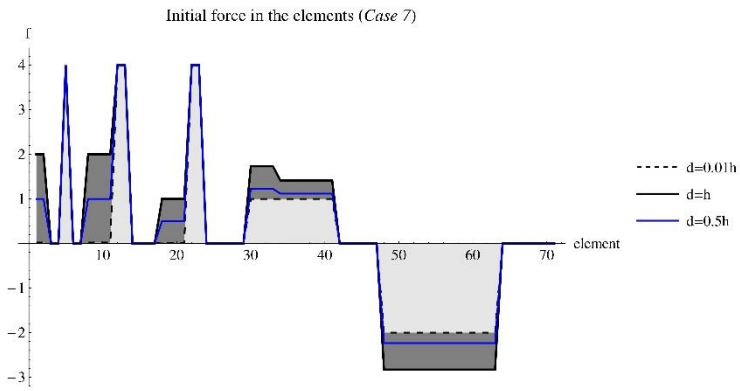

Fig. 17 Initial force vector; *Case 7* ($d \in [0.01h, h]$)

Furthermore, we show (see Figures 18-24) how the internal forces in the elements vary for d=1 and for values of h ranging from 0.01d (extremely flat grids) to d (square cell grids). In particular, the red line represents the internal force vector $\bar{\mathbf{f}}_i$ for h=0.5d.

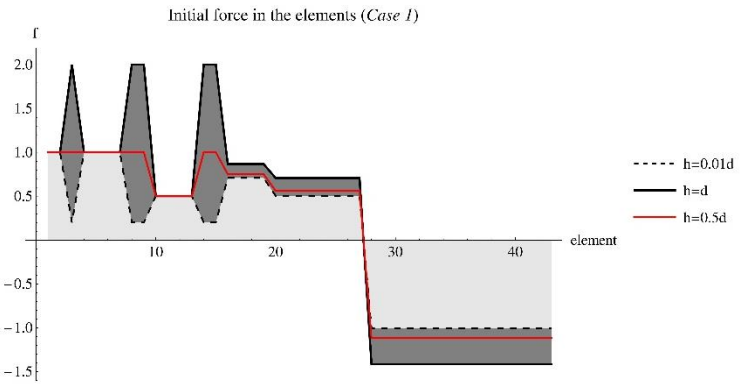

Fig. 18 Initial force vector; *Case 1* ($h \in [0.01d, d]$)

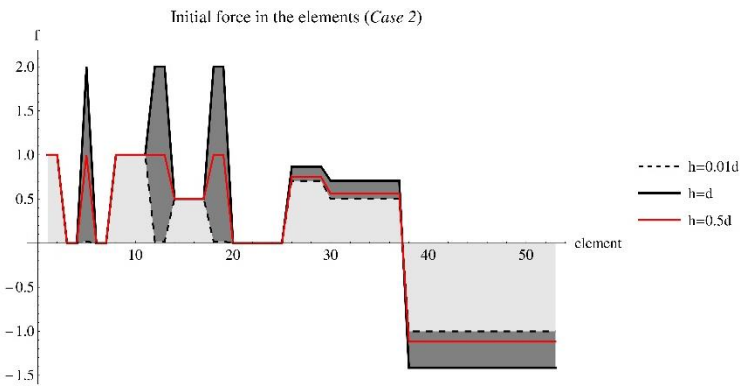

Fig. 19 Initial force vector; *Case 2* ($h \in [0.01d, d]$)

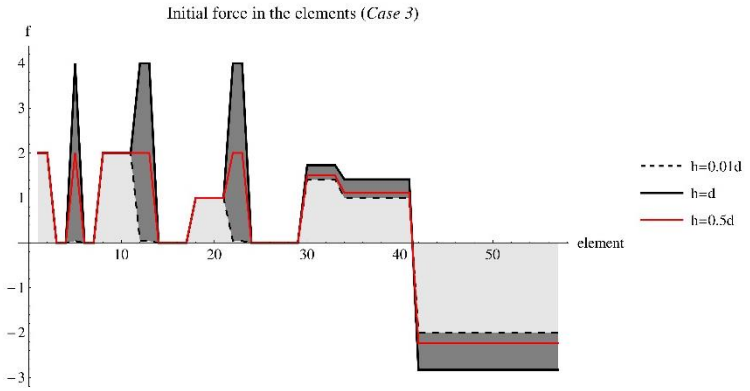

Fig. 20 Initial force vector; *Case 3* ($h \in [0.01d, d]$)

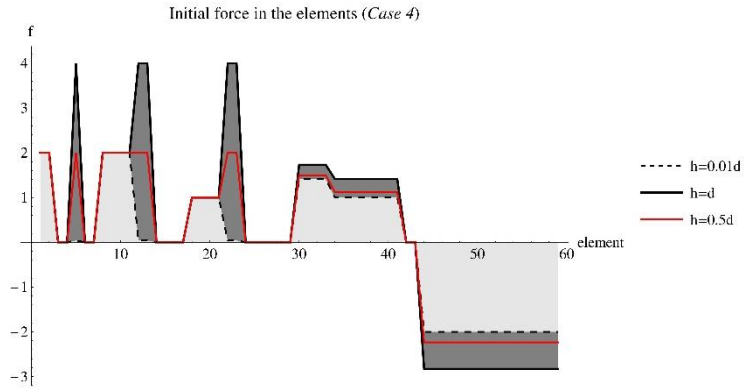

Fig. 21 Initial force vector; *Case 4* ($h \in [0.01d, d]$)

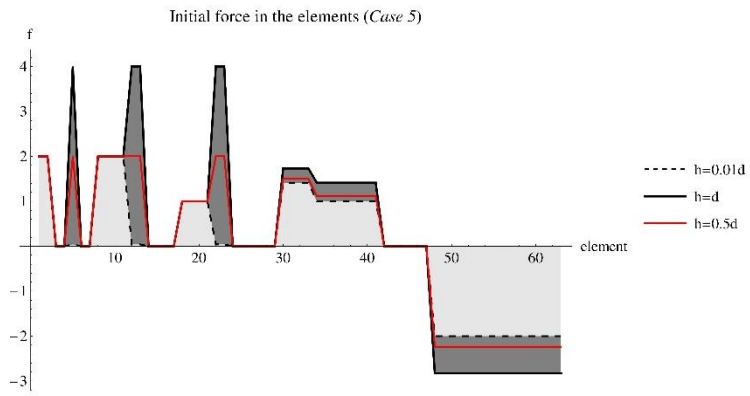

Fig. 22 Initial force vector; *Case 5* ($h \in [0.01d, d]$)

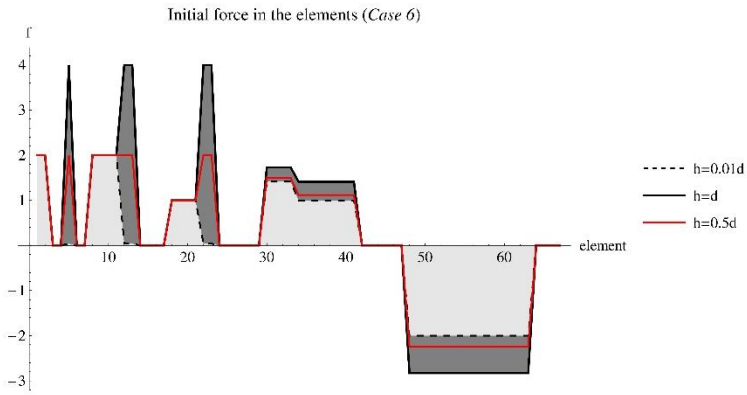

Fig. 23 Initial force vector; *Case 6* ($h \in [0.01d, d]$)

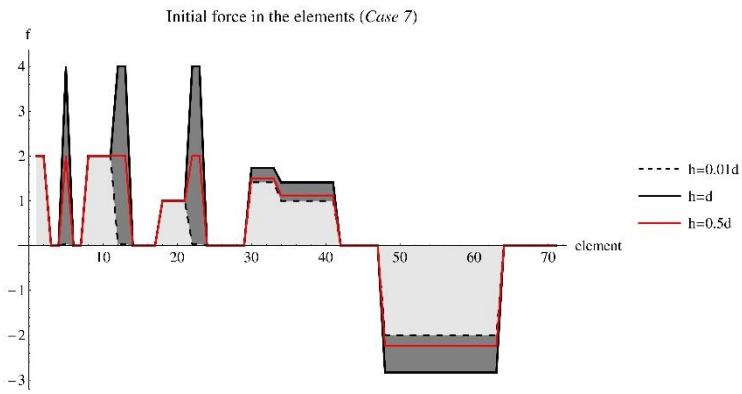

Fig. 24 Initial force vector; *Case 7* ($h \in [0.01d, d]$)

From the above, the following considerations can be pointed out:

- the force densities of all the additional elements are equal to zero, thus the internal force in these elements are zero for all the possible values of the geometric parameters d and h. Therefore, the additional elements affect the kinematical determinacy of the structure (i.e., the number of infinitesimal mechanisms reduces until it reaches zero in *Case 7*), but not the stress in the elements;
- the greater value of the tensile internal force is always obtained for the vertical cables;
- if d tends to $0.01h$, that is for extremely compact grids, the tensile internal force in the horizontal cables tends to zero; whereas if h tends to $0.01d$, that is, for extremely flat grids, the tensile internal force in vertical cables is almost zero.

5. Conclusions

We study feasible self-stress states for beam-like tensegrity grids made of V-Expander elementary cells. Our point of view is that of analyzing the influence on the feasible self-stress states of the complexification of the grid by the addition of elements, starting from

the simplest arrangement above indicated as *Case 1*. In particular, by the complexification of *Case 1* we get seven tensegrity beams, differing between them for the topology, for the number and the position of elements, but sharing the same symmetry properties. Anyway, we observe that further beams having different topologies and geometries can be generated by varying the properties of connections of the additional elements.

The main results of the performed analyses can be summarized as follows:

1. The influence of additional elements can be highlighted by the study of the null space of the equilibrium matrix, and consequently of the kernel of its transpose. In particular, we see that by adding elements the number of independent self-stress states increases. For example, we have only one independent self-stress state for *Case 1,* and 11 independent self-stress states for *Case 7*. Therefore, in the latter case the study of the feasible solution is much more complex, since we need 11 real coefficients for determining a linear combination of independent self-stress states satisfying not only the unilateral mechanical behavior of the elements, but also the symmetry properties of the structure in the self-equilibrium state.
2. Additional elements "stiffen" the V-Expander tensegrity beam: indeed, disregarding the 6 rigid-body motions, the number of infinitesimal mechanisms decreases. In particular, the kinematically indeterminate structure *Case 1* has 18 infinitesimal mechanisms, whereas *Case 7* is a kinematically determinate structure, i.e., $\bar{r}_{A^T}=0$, and then only rigid-body motions are allowed.

As a natural extension of the present work, the mechanical behavior of the analyzed V-Expander tensegrity beams under external loads may be analyzed in forthcoming studies. Also, V-Expander tensegrity beams characterized by different patterns of elements (struts and/or cables) may be investigated.

References

[1] Gilewsky W, Klosowska J, Obara P. Applications of tensegrity structures in civil engineering. Procedia Engineering, 2015; 111: 242 – 248. https://doi.org/10.1016/j.proeng.2015.07.084

[2] Gómez-Jáuregui V. Tensegrity structures and their application to architecture. Msc Dissertation, Queen's University, Belfast, 2004.

[3] Feo L, Fraternali F, Skelton RE. Composite lattices and multiscale innovative materials and structures. Composites Part B Engineering, 2016; 50(19):2995 – 3007.

[4] Skelton RE, Fraternali F, Carpentieri G, Micheletti A. Minimum mass design of tensegrity bridges with parametric architecture and multiscale complexity. Mechanics Research Communications, 2014; 58:124 – 132. https://doi.org/10.1016/j.mechrescom.2013.10.017

[5] Micheletti A. Geometrical Form-Finding of Old and New Tensegrity Modules with Orthogonal Struts. Proceedings of IASS International Symposium Shell and Spatial Structures, Venice, Italy, December, 2007.

[6] Shekastehband B, Abedi K, Chenaghlou MR. Sensitivity analysis of tensegrity systems due to member loss. Journal of Constructional Steel Research, 2011; 67: 1325 - 1340. https://doi.org/10.1016/j.jcsr.2011.03.009

[7] Fuller RB, Applewhite EJ, Loeb LA. Synergetics. Explorations in the Geometry of Thinking, Macmillan Publishing, New York, NY, USA, 1975.

[8] Harichandran A, Sreevalli IY. Form-Finding of Tensegrity Structures based on Force Density Method. Indian Journal of Science and Technology, 2016; 9: 1 - 6. https://doi.org/10.17485/ijst/2016/v9i24/93145
[9] Tran HC, Lee J. Advanced Form-finding of Tensegrity Structures. Computers & Structures, 2010; 88: 237 – 246. https://doi.org/10.1016/j.compstruc.2009.10.006
[10] Tibert AG, Pellegrino S. Review of form-finding methods for tensegrity structures. International Journal of Space Structures 2011; 26(3):241 – 255. https://doi.org/10.1260/0266-3511.26.3.241
[11] Koohestani K. On the analytical form-finding of tensegrities. Composite Structures, 2017; 166:114 – 119. https://doi.org/10.1016/j.compstruct.2017.01.059
[12] Koohestani K, Guest SD. A new approach to the analytical and numerical form-finding of tensegrity structures. International Journal of Solids and Structures, 2013; 50(19):2995 – 3007. https://doi.org/10.1016/j.ijsolstr.2013.05.014
[13] Raducanu V. Architecture et système constructif: cas des systèmes de tensègrité. Ph.D. Dissertation, Université Montpellier II, Montpellier, 2001.
[14] Motro R. Tensegrity: Structural Systems for the Future, Kogan page Science, London, UK, 2003.
[15] Zhang JY, Ohsaki M. Stability conditions for tensegrity structures. International Journal of Solids and Structures, 2007; 44, 3875 – 3886. https://doi.org/10.1016/j.ijsolstr.2006.10.027
[16] Lee S, Lee J. A novel method for topology design of tensegrity structures. Composite Structures, 2016; 152:11 – 19. https://doi.org/10.1016/j.compstruct.2016.05.009
[17] Scheck HJ. The force density method for form finding and computation of general networks. Computer Methods in Applied Mechanics and Engineering, 1974; 3: 115 – 134. https://doi.org/10.1016/0045-7825(74)90045-0
[18] Juan SH, Tur JMM. Tensegrity frameworks: static analysis review. Mechanism and Machine Theory, 2008; 43(7):859 – 81. https://doi.org/10.1016/j.mechmachtheory.2007.06.010
[19] Tran HC, Lee J. Self-stress design of tensegrity grid structures with exostresses. International Journal of Solids and Structures, 2010; 47:2660 – 2671. https://doi.org/10.1016/j.ijsolstr.2010.05.020
[20] Tran HC, Lee J. Initial self-stress design of tensegrity grid structures. Computers & Structures, 2010; 88: 558 – 566. https://doi.org/10.1016/j.compstruc.2010.01.011
[21] Koohestani K. Form-finding of tensegrity structures via genetic algorithm. International Journal of Solids and Structures, 2012; 49(5):739 – 747. https://doi.org/10.1016/j.ijsolstr.2011.11.015
[22] Raducanu V, Motro R. Stable self-balancing system for building component, Demande de brevet français n. 01 04 822, 2002.
[23] Skelton RE, de Oliveira MC. Tensegrity Systems, New York: Springer Science+Business Media, 2009.
[24] Pinaud JP, Solari S, Skelton RE. Deployment of a class 2 tensegrity boom. Proceedings of SPIE - The International Society for Optical Engineering, Jult, 2004. https://doi.org/10.1117/12.540150
[25] Cheong J, Skelton RE. Nonminimal Dynamics of General Class k Tensegrity Systems. International Journal of Structural Stability and Dynamics, 2015; 15(2): 1450042-1 - 1450042-22.
[26] Böhm V, Sumi S, Kaufhold T, Zimmermann K. Compliant Multistable Tensegrity Structures with Simple Topologies. New Trends in Mechanism and Machine Science, Springer, 2017; 43: 153 – 161. https://doi.org/10.1007/978-3-319-44156-6_16
[27] Guo J, Jiang J. An algorithm for calculating the feasible pre-stress of cable-struts structure. Engineering Structures, 2016; 118: 228 – 239. https://doi.org/10.1016/j.engstruct.2016.03.058

[28] Chen Y, Feng J, Liu Y. A group-theoretic approach to the mobility and kinematic of symmetric over-constrained structures. Mechanism and Machine Theory, 2016; 105: 91 – 107. https://doi.org/10.1016/j.mechmachtheory.2016.06.004

[29] Motro R. Tensarch: A tensegrity double layer grid prototype. Space Structures, 2002; 5:31-38. https://doi.org/10.1680/ss5v1.31739.0007

[30] Foti P, Fraddosio A, Marzano S, Pavone G, Piccioni MD. On self-stress design in modular tensegrity grid structures. Proceedings of 11th International Conference on Applied and Theoretical Mechanics (MECHANICS '15), Kuala Lumpur, Malaysia, April, 2015.